American Journal of Climate Change, 2025, 14(2), 248-270
https://www.scirp.org/journal/ajcc
ISSN Online: 2167-9509
ISSN Print: 2167-9495

Blue Carbon Sequestration Potential of Soils in Degraded Mangroves of Sundarban, India: A Geochemical Approach

Anubhav Das[1,2], Pratap Bhattacharyya[1*], Somnath Khaoash[2], Sujit Kumar Nayak[1], Shiva Prasad Parida[1], Soumya Ranjan Padhy[1], Sarada Prasad Pradhan[3]

[1]Crop Production Division, ICAR-National Rice Research Institute, Cuttack, Odisha, India
[2]Department of Geology, Ravenshaw University, Cuttack, Odisha, India
[3]Department of Earth Sciences, Indian Institute of Technology Roorkee, Roorkee, Uttarakhand, India
Email: *pratap162001@gmail.com

How to cite this paper: Das, A., Bhattacharyya, P., Khaoash, S., Nayak, S. K., Parida, S. P., Padhy, S. R., & Pradhan, S. P. (2025). Blue Carbon Sequestration Potential of Soils in Degraded Mangroves of Sundarban, India: A Geochemical Approach. *American Journal of Climate Change, 14,* 248-270.
https://doi.org/10.4236/ajcc.2025.142013

Received: January 30, 2025
Accepted: May 16, 2025
Published: May 19, 2025

Abstract

Mangrove ecosystems are important for global carbon sequestration, with their soils storing approximately 1.71 ± 0.17 Mg C ha^{-1} yr^{-1} of organic carbon. However, these ecosystems face challenge of degradation at a rate of nearly 42% as observed in the past decade in India. Moreover, degraded mangroves have become an integral part of the wetland ecosystems in Sundarbans. In this study, we investigate the geochemical interactions influencing soil carbon sequestration potential in degraded mangrove soils of the Indian Sundarbans. Soil samples were collected from three major estuaries: Bidyadhari, Hooghly and Matla up to 5 metre depths (at 1 m interval) with replications. Samples were analysed for total carbon (TC), soil organic carbon (SOC), major oxide compositions, trace element concentrations, and clay minerals. TC (0.67 - 0.94%) and SOC (0.58 - 0.73%) showed highest concentrations at 0 - 1 m soil depth due to greater organic inputs and declined with depth across all sites. Silicon dioxide (46% - 51%) and aluminium oxide (18% - 23%) were observed in higher concentrations across all sites which may contribute to clay-humus complexes with the potential to stabilize organic carbon. Trace elements showed stratified distributions influenced by redox cycling, tidal inputs, and anthropogenic inputs, particularly in Hooghly and Bidyadhari estuaries. Presence of Chromium (Cr), manganese (Mn) and zinc (Zn) indicated the potential to form insoluble oxides and hydroxides that could act as adsorption sites for organic carbon, thereby enhancing its stability. Secondary clay minerals like glauconite and argentopyrite indicated stable soil matrices that further supported carbon stabilization. This study emphasizes the geochemical characteristics of Sundarban degraded mangrove system in relation to carbon sequestration potential and

factors influencing the soil carbon dynamics.

Keywords

Mangrove Ecosystems, Carbon Sequestration, Geochemical Interactions, Degraded Soils, Trace Elements

1. Introduction

Mangrove ecosystems, situated in the intertidal zones of tropical and subtropical regions, are globally recognized for their remarkable ability to sequester carbon, commonly referred to as blue carbon (Alongi, 2012; Kauffman et al., 2020). These ecosystems play a critical role in mitigating climate change by capturing atmospheric carbon dioxide (CO_2) and storing it within their biomass and soils (Choudhary et al., 2024; Donato et al., 2011). The Sundarbans are the world's largest contiguous mangrove forest spanning approximately 10,200 km^2, of which 38% is in India and remaining in Bangladesh (Spalding, 2010). This area is characterized by high biodiversity, extensive tidal channels, and mudflats that are influenced by dynamic tidal fluctuations, which affect biogeochemical processes important to carbon sequestration (Al Mahmud et al., 2024; Padhy et al., 2023). Sundarban mangroves contribute substantially to regional and global carbon cycles with estimated carbon sequestration rates ranging from 4.71 to 6.54 Mg C ha^{-1} yr^{-1} (Ray et al., 2021). Key areas include the South 24 Parganas Reserve Forest, spanning 1678 km^2, and the Sundarban Tiger Reserve, covering 2585 km^2. Nearly 13% of these mangroves have been degraded during 1930-2024 due to climate change vagaries and land conversion for rice cultivation and aquaculture systems. This degraded mangrove system, interspersed with rice paddies and aquaculture ponds and subjected to intense anthropogenic pressure, represents a unique ecological matrix prevalent in the Indian Sundarban region. Due to the dense human population and associated socio-demographic constraints, restoring these degraded areas to pristine or core mangrove forests is extremely challenging. Moreover, as the Sundarbans have been designated as a reserve forest, the current land-use configuration—comprising degraded mangroves, rice fields, and aquaculture—is expected to persist in the coming decades. Over the last century, 40% of tropical mangroves globally have been lost, with a significant portion becoming ecologically degraded (Padhy et al., 2020). The Indian Sundarban mangroves constitute approximately 2.84% of the world's total mangrove area. The Sundarbans biosphere acts as a net carbon sink, sequestering 2.79 teragrams of carbon (Tg C) annually, with around 96% of this carbon stored in below-ground biomass, while the remainder is retained in above-ground biomass (Nayak et al., 2024; Ray et al., 2013).

Although degraded mangrove ecosystems have lower carbon sequestration capacity than core or undisturbed mangroves, they still exhibit higher carbon stor-

age potential than adjacent rice-aquaculture systems. Several studies (Padhy et al., 2021; Royna et al., 2024) indicate that with sustained conservation efforts and replantation strategies, even degraded mangrove systems can outperform rice-aquaculture landscapes in terms of carbon storage. Hence, this mosaic of degraded mangroves, though suboptimal compared to pristine forests, holds relatively higher carbon sequestration potential than surrounding non-mangrove land uses.

However, the geochemical processes influencing the stabilization of soil organic carbon (SOC), particularly through trace elements and elemental oxides, are not fully understood. Elemental oxides like sodium oxide (Na_2O), magnesium oxide (MgO), aluminium oxide (Al_2O_3), silicon dioxide (SiO_2), phosphorus pentoxide (P_2O_5), sulphur trioxide (SO_3), potassium oxide (K_2O), calcium oxide (CaO), titanium dioxide (TiO_2), and ferric oxide (Fe_2O_3) play a vital role in blue carbon characterization (Cai et al., 2024; Murugesan et al., 2021; Romero-Mujalli & Melendez, 2023). These oxides influence soil mineralogy, pH, and redox potential that are critical for carbon stabilization. Fe_2O_3 and Al_2O_3 stabilize organic matter through clay-humus complex formation, while SiO_2 and TiO_2 enhance organic carbon retention via adsorption surfaces (Frates et al., 2023; Li et al., 2023).

Carbon sequestration in mangrove soils is driven by complex interactions among soil organic matter (SOM), mineralogy, and trace element geochemistry, which together influence carbon stabilization mechanisms. Trace elements such as chromium (Cr), manganese (Mn), nickel (Ni), copper (Cu), zinc (Zn), cadmium (Cd), and lead (Pb) influence carbon stabilization. These elements can form complexes with organic matter or precipitate as insoluble compounds under anoxic conditions that prevail in mangrove soils (Wang et al., 2024a; Wu et al., 2024). Cr and Pb, for instance, stabilize SOC through adsorption, while Mn, Ni, and Cu catalyse microbial and enzymatic processes that affect carbon turnover (Grey et al., 2023; Ray et al., 2023).

The spatial distribution of trace elements and elemental oxides in mangrove soils is strongly stratified, with higher concentrations typically observed in surface layers (0 - 1 m) due to atmospheric deposition, tidal inputs, and anthropogenic activities. Elements such as Cu, Zn, and Cd are frequently enriched in surface soils, while concentrations decline with depth due to vertical leaching and redox-induced immobilization (Rahman et al., 2024).

In the Indian Sundarbans, anthropogenic activities such as industrial effluents, agricultural runoff, urbanization, and shipping have significantly altered degraded mangrove system's soil geochemistry. Recent studies highlight trace metal enrichment, including Cr, Mn, Ni, Cu, Zn, Cd, and Pb, emphasizing the impact of industrial and agricultural activities (Islam et al., 2022; Sharma et al., 2021). Higher concentrations of specific trace element concentrations and their interactions with oxides like Fe_2O_3 and TiO_2 reveal complex carbon stabilization mechanisms (Li et al., 2023).

Tidal-driven redox cycling affects trace element movement and reactivity, as the periodic oxidation and reduction of Fe and Mn compounds release and re-

adsorb organic matter and trace elements, helping stabilize SOC in deeper layers (Queiroz et al., 2022; Tognella et al., 2016). The effect of tidal influence varied among the estuaries and distance from the sea (Bhattacharyya et al., 2023). However, majority of studies (Cooray et al., 2024; Grey et al., 2023; Rovai et al., 2018) focus on surface soils (0 - 1 m), overlooking significant carbon stocks in deeper layers. Mangrove soils extending to deeper soils (5 metres or so) offer unique insights into the potential of long-term carbon sequestration. Depth-resolved studies are critical for quantifying total carbon (TC) storage and understanding stabilization mechanisms, especially given the vulnerability of deep soils to environmental disturbances like land-use and hydrological changes (Sierra et al., 2024).

This study comprehensively investigates the role of trace elements and elemental oxides in the stabilization of soil organic carbon (SOC) within Sundarban mangrove soils, extending to a depth of 5 meters. To achieve the quantified data and correlation between SOC, elemental oxides and trace elements, depth-wise soil samples were considered from the three major estuaries of Sundarbans, representing distinct geological background and anthropogenic activities. The findings unveil critical geochemical interactions driving SOC stabilization, offering a transformative framework for advancing blue carbon accounting and global carbon management.

2. Methodology

2.1. Study Area and Site Selection

The study was conducted in the degraded mangroves of Indian Sundarban located at three different estuarine systems. The research focused on three river estuarine systems selected based on their drainage patterns, sedimentation rates, and depositional environments: Dayapur (22˚08'02.3" N 88˚50'37.7" E) along Bidyadhari estuarine, Sagar Island (21˚46'15.2" N 88˚10'09.3" E) along Hooghly estuarine and Maipith (21˚51'58.3" N 88˚30'39.7" E) along Matla estuarine (**Figure 1**). At each location, four sampling sites were chosen to acquire variability arising from both natural environmental gradients and anthropogenic influences. These locations were chosen because they reflect a broad range of environmental conditions, including differences in geology, salinity, mangrove species, tidal patterns, and the extent of human impact. This variety helps us better understand how these factors influence geochemical processes related to carbon storage. While our study offers a snapshot in time, it serves as a valuable starting point for assessing the carbon sequestration potential of degraded mangrove systems in the region.

2.2. Soil Sampling

Soil samples were collected from the surface to a depth of 5 meters using a combination of soil augers and manual excavation. Sampling was performed at 1-meter intervals to capture variations in carbon and geochemical properties across the vertical profile. A total of 12 locations (four from each estuarine site) were sam-

pled to ensure comprehensive spatial representation. The collected samples were air-dried, sieved through 2 mm mesh (0.5 mm sieve was used for total carbon analysis), and homogenized before undergoing laboratory analyses.

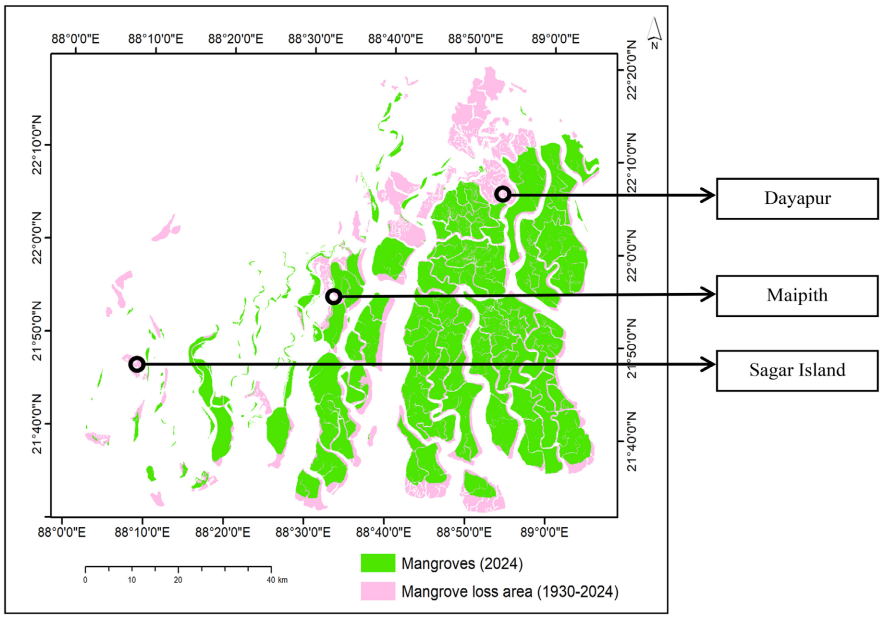

Figure 1. Map showing the three study areas (Dayapur along Bidyadhari estuarine, Sagar Island along Hooghly estuarine and Maipith along Matla estuarine) and the degradation of mangroves from 1930 to 2024 in Sundarban, India.

2.3. Carbon and Geochemical Analyses

2.3.1. Soil Organic Carbon (SOC) and Total Carbon (TC)

The SOC was determined using the Walkley-Black method, a dichromate oxidation technique widely employed for soil analysis. Total carbon (TC) was measured by dry combustion method using an AnalytikJena Multi N/C 2100S analyzer.

2.3.2. Major Oxides and Trace Element Estimation

The geochemical composition of the soils was analyzed using two techniques, namely X-ray fluorescence (XRF) and Inductively Coupled Plasma Mass Spectrometry (ICP-MS). XRF analysis was done to quantify the major oxide percentages, including sodium oxide (Na_2O), magnesium oxide (MgO), aluminium oxide (Al_2O_3), silicon dioxide (SiO_2), phosphorus pentoxide (P_2O_5), sulphur trioxide (SO_3), potassium oxide (K_2O), calcium oxide (CaO), titanium dioxide (TiO_2), and ferric oxide (Fe_2O_3). The ICP-MS analysis was performed to determine the concentrations of trace elements like chromium (Cr), manganese (Mn), nickel (Ni), copper (Cu), zinc (Zn), cadmium (Cd), and lead (Pb).

2.3.3. Clay Mineralogy Identification

X-ray Diffraction (XRD) analysis was done to identify dominant clay minerals. Samples from three depths i.e., 1 m, 2.5 m, and 5 m, were analysed for each site. The analysis used a Cu K-α radiation source, operating at 40 kV and 40 mA,

with a scanning rate of 4˚/minute. Diffractogram-derived "d" values were matched against the Joint Committee on Powder Diffraction Standards (JCPDS) database using X'pert HighScore Plus (v3.1) software for precise mineral identification.

2.4. Data Analysis

To evaluate spatial and vertical variability in the studied parameters, a two-factor analysis of variance (ANOVA) was performed using the OPSTAT online software. Depth and location were treated as independent variables, with a significance threshold of $p \leq 0.05$. The depth-wise variation data analysis was done in RStudio (v2021.09.2). The correlation analyses were done in RStudio (v2021.09.2) using corrplot package.

3. Results

3.1. Soil Carbon Distribution across Depths

The distribution of total carbon (TC) and soil organic carbon (SOC) in 1m to 5m soil profile varied across the studied sites. TC concentrations were highest in surface soils (0 - 1 m), with Maipith (Matla estuarine) recording the maximum value of 0.94%, followed by Sagar Island (Hooghly estuarine, 0.75%) and Dayapur (Bidyadhari estuarine, 0.67%) (Figure 2). TC was found to be decreasing with increasing depth across all the sites. At 4 - 5 m depth, TC values were 0.50% at Maipith, 0.72% at Sagar Island and 0.65% at Dayapur. Similarly, SOC levels were highest in the uppermost layers (0 - 1 m), with Maipith reaching 0.73% in surface soils (Figure 3). SOC values decreased progressively with depth, showing the lowest values at 4 - 5 m (0.41% at Maipith, 0.42% at Sagar Island, and 0.59% at Dayapur). Despite site-specific differences, all locations exhibited a consistent declining trend in carbon concentrations with depth.

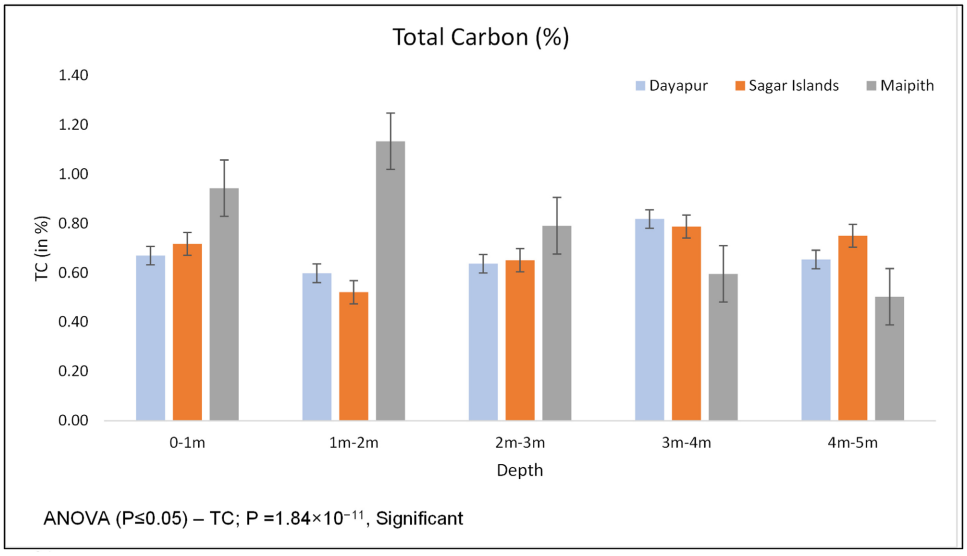

Figure 2. Depth-wise and site-wise variation of Total Carbon.

3.2. Variation of Oxide Composition and Concentration

Oxide composition and concentration varied with soil depths among the three study sites located in three distinct estuaries (Figure 4). Silicon dioxide (SiO_2) was the predominant oxide, with its concentration increasing with depth at all sites. Surface soils (0 - 1 m) displayed the highest SiO_2 concentrations at Maipith (Matla estuarine, 51%), followed by Sagar Island (Hooghly estuarine, 49.2%) and Dayapur (Bidyadhari estuarine, 45.7%). SiO_2 exhibited relatively higher concentrations at deeper depths (4 - 5 m) in Maipith (60.2%) and Sagar Island (58.9%) compared to Dayapur (51.3%).

Ferric oxide (Fe_2O_3) was most concentrated at surface soils (0 - 1 m) but gradually decreased with depth. At the surface layer (0 - 1 m), Fe_2O_3 concentration

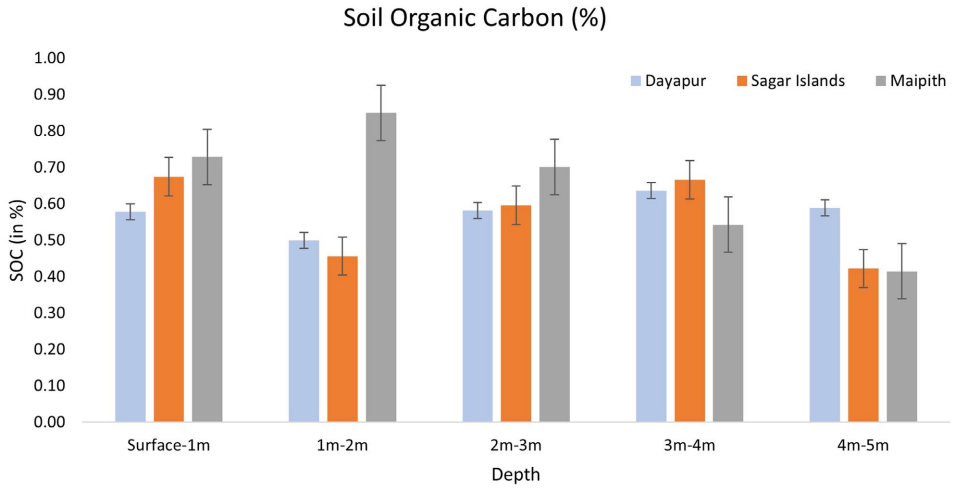

Figure 3. Depth-wise and site-wise variation of Soil Organic Carbon.

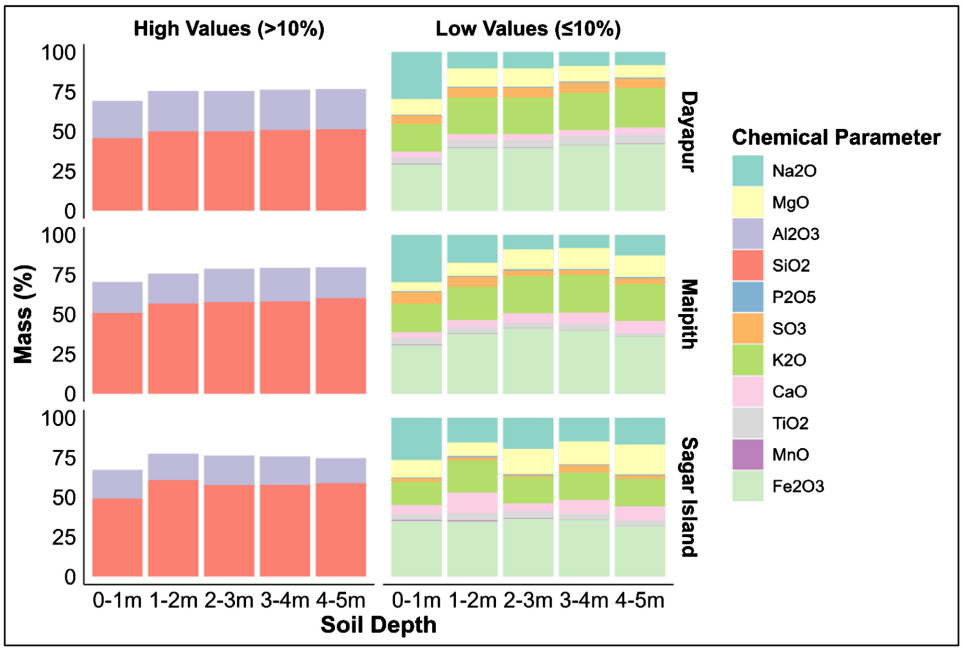

Figure 4. Variation of oxide concentrations along different depth at the three locations.

was highest at Sagar Island (8.9%) followed by Maipith (7.3%) and Dayapur (6.4%). At 4 - 5 m depth, Fe_2O_3 concentrations were highest at Sagar Island (7.3%), followed by Dayapur (6.9%) and Maipith (6.9%). Fe_2O_3 concentrations varied across depths, with peak values observed at Maipith (8% at 2 - 3 m soil depth) and Sagar Island (8.2% at 3 - 4 m soil depth).

Surface soils (0 - 1 m) recorded the highest Na_2O concentrations at Maipith (Matla estuarine, 7.1%), followed by Sagar Island (Hooghly estuarine, 6.7%) and Dayapur (Bidyadhari estuarine, 6.5%). Na_2O concentrations declined sharply with depth at all sites, reaching their lowest values at 4 - 5 m, with 3.8% at Sagar Island, followed by 2.5% at Maipith and 1.4% at Dayapur.

Surface soils (0 - 1 m) showed the highest Al_2O_3 concentration at Dayapur (Bidyadhari estuarine, 23.6%), followed by Maipith (Matla estuarine, 19.5%) and Sagar Island (Hooghly estuarine, 18.1%). At 4 - 5 m depth, Al_2O_3 was again highest at Dayapur (25.3%), followed by Maipith (19.5%) and Sagar Island (15.7%). Al_2O_3 consistently increased with depth at Dayapur, with lower but relatively stable values at Maipith and Sagar Island.

At surface layer (0 - 1 m), K_2O concentrations were highest at Maipith (Matla estuarine, 4.3%), followed by Dayapur (Bidyadhari estuarine, 3.8%) and Sagar Island (Hooghly estuarine, 3.7%). At 4 - 5 m depth, K_2O concentrations were highest at Maipith (4.4%), followed by Dayapur (4.1%) and Sagar Island (3.9%). K_2O showed a gradual increase with depth at all sites.

Phosphorus pentoxide (P_2O_5) exhibited minor concentrations, ranging from 0.11 - 0.14%, while other oxides, including magnesium oxide (MgO) and calcium oxide (CaO), showed minimal fluctuations across the depths in all studied sites. These trends indicate the potential role of site-specific factors in shaping the vertical distribution of major oxides.

The correlation analysis between Soil Organic Carbon (SOC) and major soil oxides reveals distinct trends across the dataset (**Figure 5**). A strong positive correlation was observed between SOC and SO_3 ($r \approx 0.56$), followed by a moderate correlation with Fe_2O_3 ($r \approx 0.51$) and TiO_2 ($r \approx 0.36$). SOC content also showed a weak positive trend with MnO ($r \approx 0.17$) and Al_2O_3 ($r \approx 0.04$). In contrast, SOC exhibited a clear negative correlation with SiO_2 ($r \approx -0.26$), and no significant correlation was observed with K_2O. These patterns suggest that the distribution of SOC is closely associated with specific oxide concentrations, particularly those of iron, sulphur and aluminium.

3.3. Trace Elements Composition and Concentrations

Trace element concentrations varied notably with soil depth among the three study sites, reflecting the influence of site-specific geochemical processes (**Figure 6**). Surface soils (0 - 1 m) exhibited the highest Cr concentrations at Dayapur (Bidyadhari estuarine, 89.2 ppm), followed closely by Sagar Island (Hooghly estuarine, 89.1 ppm) and Maipith (Matla estuarine, 88.3 ppm). At 4 - 5 m depth, Cr concentrations were highest at Sagar Island (80.8 ppm), followed by Maipith (54.4

ppm) and Dayapur (52.5 ppm). With increasing depth, Cr concentrations generally declined at all sites, reaching the lowest values at Maipith (49.5 ppm at 3 - 4 m) and Dayapur (52.4 ppm at 4 - 5 m). Sagar Island displayed higher (95.2 ppm) Cr values at 2 - 3 m depth.

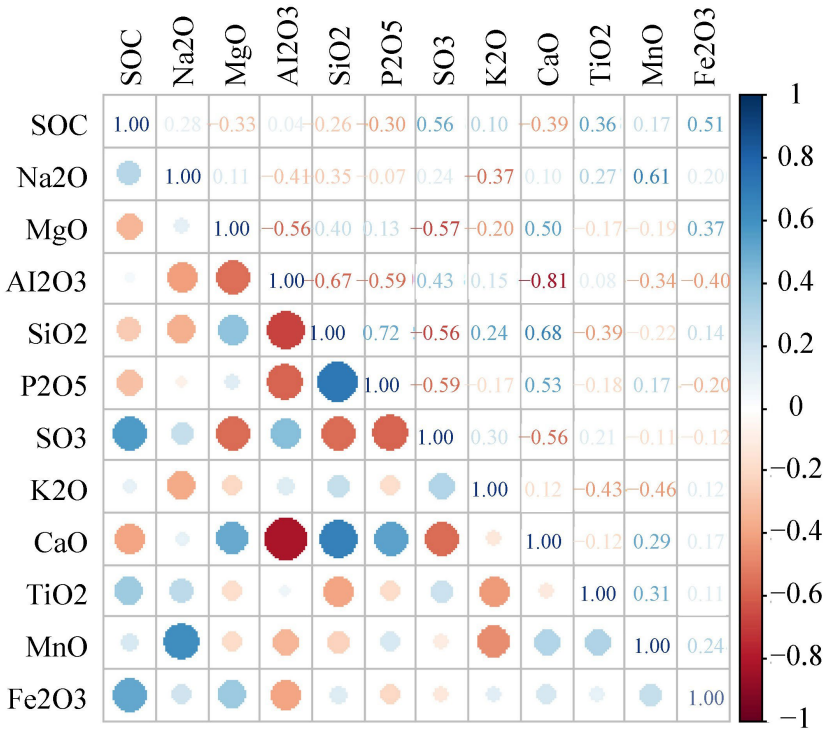

Figure 5. Pearson correlation matrix between Soil Organic Carbon (SOC) content and major oxides (Fe_2O_3, Al_2O_3, SiO_2, TiO_2, CaO, MgO, MnO) in mangrove soils at all three study areas. Shades of blue represent positive correlations, while red shades indicate negative correlations. The colour intensity and the circular sizes reflect the strength of correlation, with values ranging from −1 to +1.

Manganese (Mn) concentrations were highest in surface soils (0 - 1 m) at Sagar Island (Hooghly estuarine, 696.1 ppm), followed by Dayapur (Bidyadhari estuarine, 553 ppm) and Maipith (Matla estuarine, 279.6 ppm). At 4 - 5 m depth, Mn concentrations were highest at Sagar Island (615.4 ppm), followed by Dayapur (241.6 ppm) and Maipith (238.1 ppm). With depth, Mn concentration declined sharply, reaching minimum values at Maipith (171 ppm at 3 - 4 m) and Dayapur (241.6 ppm at 4 - 5 m). However, Sagar Island consistently showed higher Mn concentration across all depths with maximum (787.7 ppm) at 1 - 2 m depth interval.

Nickel (Ni) concentrations in surface soils (0 - 1 m) were highest at Sagar Island (Hooghly estuarine, 49 ppm), followed by Dayapur (Bidyadhari estuarine, 46.7 ppm) and Maipith (Matla estuarine, 43.4 ppm). At 4 - 5 m depth, Ni concentrations were highest at Sagar Island (44.5 ppm), followed by Maipith (27.5 ppm) and Dayapur (21.8 ppm). Ni concentrations showed a decreasing trend with depth, with the lowest values observed at Dayapur (21.8 ppm at 4 - 5 m) and Maipith (23.6 ppm at 3 - 4 m).

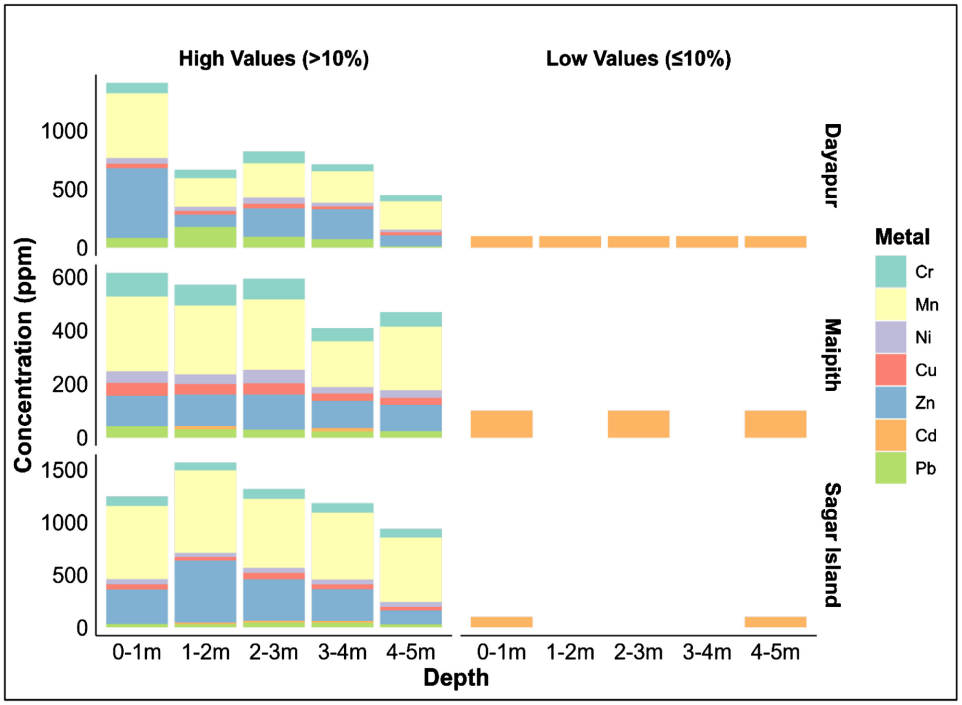

Figure 6. Variation of trace element concentration along different depths at the three locations.

Copper (Cu) concentrations in surface soils (0 - 1 m) were highest at Sagar Island (Hooghly estuarine, 50.5 ppm), followed by Maipith (Matla estuarine, 47.9 ppm) and Dayapur (Bidyadhari estuarine, 40.1 ppm). At 4 - 5 m depth, Cu concentrations were highest at Sagar Island (35.6 ppm), followed by Maipith (27.1 ppm) and Dayapur (26.6 ppm). With increasing depth, Cu concentration declined, reaching minimum values at Dayapur (25.3 ppm at 3 - 4 m) and Maipith (27.1 ppm at 4 - 5 m). Sagar Island maintained higher (60.2 ppm) Cu concentrations at 2 - 3 m depth.

Zinc (Zn) concentrations in surface soil (0 - 1 m) were highest at Dayapur (Bidyadhari estuarine, 595.1 ppm), followed by Sagar Island (Hooghly estuarine, 327.8 ppm) and Maipith (Matla estuarine, 113.9 ppm). At 4 - 5 m depth, Zn concentrations were highest at Sagar Island (131.8 ppm), followed by Maipith (97.8 ppm) and Dayapur (94.5 ppm). Zn concentration declined with depth, reaching minimum values at Dayapur (94.5 ppm at 4 - 5 m) and Maipith (97.8 ppm at 4 - 5 m). Sagar Island maintained moderate Zn levels, showing peak value (394.7 ppm) at 2 - 3 m.

Cadmium (Cd) concentrations in surface soil (0 - 1 m) were highest at Dayapur (Bidyadhari estuarine, 9.7 ppm), followed closely by Maipith (Matla estuarine, 9.1 ppm) and Sagar Island (Hooghly estuarine, 7.8 ppm). At 4 - 5 m, Cd concentrations were highest at Maipith (7.2 ppm), followed by Sagar Island (5.1 ppm) and Dayapur (3.8 ppm). Cd concentration peaked at mid-depths (2 - 3 m) in Sagar Island (16.8 ppm) but generally declined with depth across all sites.

Lead (Pb) concentrations in surface soils (0 - 1 m) were highest at Dayapur (Bidyadhari estuarine, 82.9 ppm), followed by Maipith (Matla estuarine, 42.3

ppm) and Sagar Island (Hooghly estuarine, 33.1 ppm). At 4 - 5 m depth, Pb concentrations were highest at Sagar Island (29.4 ppm), followed by Maipith (24.1 ppm) and Dayapur (11.5 ppm). Pb concentrations declined with depth, reaching the lowest values at Dayapur (11.5 ppm at 4 - 5 m) and Maipith (22.9 ppm at 3 - 4 m). Sagar Island showed relatively stable Pb concentrations, with the highest value of 46.8 ppm at 2 - 3 m.

The correlation matrix (Figure 7) revealed several notable relationships between Soil Organic Carbon (SOC) and trace elements in Sundarban mangrove soils. A strong positive correlation was observed between SOC and Copper (Cu) ($r \approx 0.43$), indicating a substantial association. Nickel (Ni) also showed moderate to strong positive correlations with SOC ($r \approx 0.26$). In contrast, Manganese (Mn), Zinc (Zn), and Lead (Pb) exhibited weak or negligible correlations with SOC, suggesting minimal co-variation.

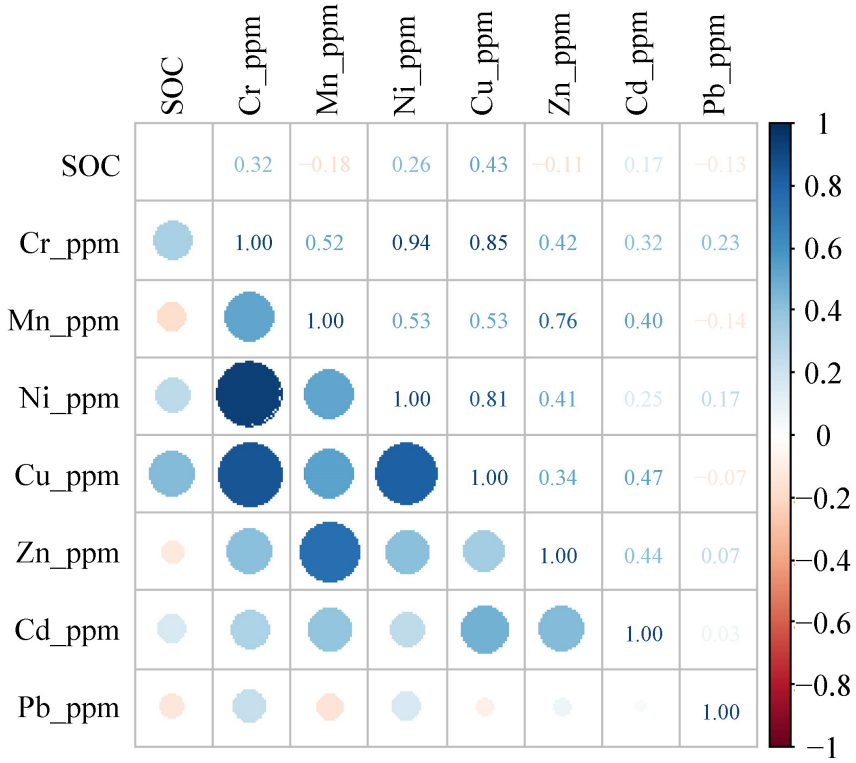

Figure 7. Pearson correlation matrix between Soil Organic Carbon (SOC) and selected trace elements (Fe, Mn, Zn, Cu, Cr, Ni, Pb, Ti, and Cd) in mangrove soils at all three study areas. Shades of blue represent positive correlations, while red shades indicate negative correlations. The colour intensity and the circular sizes reflect the strength of correlation, with values ranging from –1 to +1.

3.4. Variation of Clay Mineral Composition

At 1 m depth, glauconite was consistently detected across all three estuarines (Figure 8(a), Figure 8(d), Figure 8(g)). At 5 m depth, argentopyrite and pyrite were prominent across all sites (Figure 8(c), Figure 8(f), Figure 8(i)). Distinct site-specific minerals were observed at intermediate and deeper depths. At 2.5 m

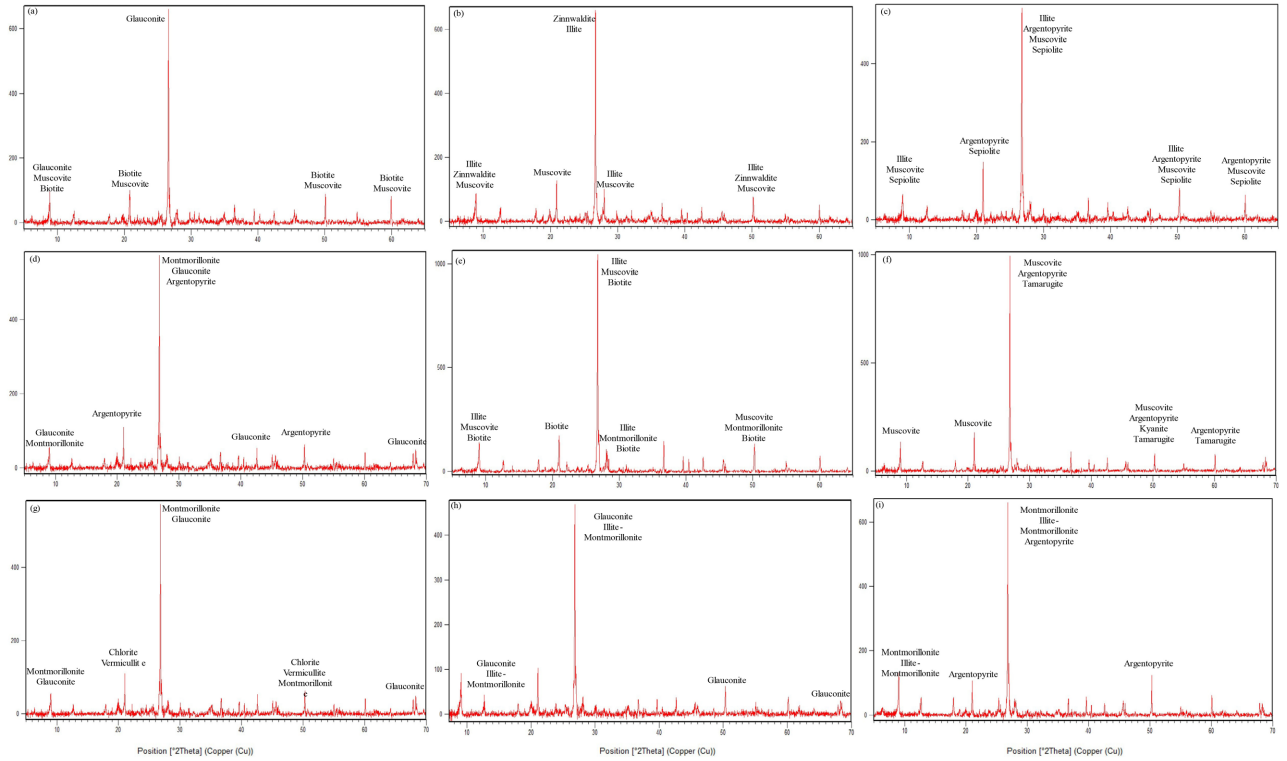

Figure 8. XRD diffractograms depicting the clay mineralogy of soil samples collected from different depths across three study areas: (a) Dayapur, 1 m depth; (b) Dayapur, 2.5 m depth; (c) Dayapur, 5 m depth; (d) Sagar Island, 1 m depth; (e) Sagar Island, 2.5 m depth; (f) Sagar Island, 5 m depth; (g) Maipith, 1 m depth; (h) Maipith, 2.5 m depth; (i) Maipith, 5 m depth.

depth in Dayapur (Bidyadhari estuarine), zinnwaldite, a lithium-rich mica, was detected (**Figure 8(b)**). In the 5 m soil sample from Dayapur (Bidyadhari estuarine), sepiolite, a magnesium-rich silicate, was identified (**Figure 8(c)**). Soil samples at a depth of 5 meters in Sagar Island (Hooghly estuarine) revealed the presence of tamarugite, a sodium aluminium sulphate mineral (**Figure 8(f)**). In Maipith (Matla estuarine), chlorite-vermicullite was identified at a depth of 1 meter, indicating partial weathering of chlorite under alternating wet and dry conditions (**Figure 8(g)**). At a depth of 5 meters in Maipith (Matla estuarine), argentopyrite and montmorillonite were detected (**Figure 8(i)**).

3.5. Mangrove Species Distribution and Density Patterns across Estuarine Systems

The comparative assessment of mangrove species density across three estuarine systems—Dayapur (Bidyadhari estuary), Sagar Island (Hooghly estuary), and Maipith (Matla estuary)—revealed prominent differences in species composition and total vegetation density (independent tree ha^{-1}) (**Table 1**). Dayapur exhibited the highest species richness (six species), followed by Sagar Island and Maipith, each with five species. Among the studied species, *Avicennia alba* demonstrated pervasive presence and dominance across all sites, with the highest density observed at Dayapur (1092.59 Ind. ha^{-1}), followed by Sagar Island (722.22 Ind. ha^{-1}) and Maipith (703.70 Ind. ha^{-1}). *Avicennia officinalis* was the second most preva-

lent species, present across all sites with a moderately high density. In contrast, *Ceriops decandra* was exclusively recorded at Dayapur with a low density of 127.78 Ind. ha^{-1}). *Sagar Island* recorded the highest total vegetation density (2677.77 Ind. ha^{-1}), primarily attributed to the overwhelming dominance of *Sonneratia apetala* (1044.44 Ind. ha^{-1}). This species was absent in Dayapur but found in both Sagar Island and Maipith, indicating site-specific preference. Notably, *Avicennia marina* was exclusively found in Maipith (244.44 Ind. ha^{-1}), reflecting localized environmental conditions conducive to its establishment.

Table 1. Spatial distribution and species-wise density (individuals per hectare) of dominant mangrove species across the three estuarine systems—Bidyadhari (Dayapur), Hooghly (Sagar Island), and Matla (Maipith)in Sundarban, India.

Site	Estuarine System	Coordinates	Species	Density (Ind ha^{-1})
Dayapur	Bidyadhari	22˚08'02.3" N 88˚50'37.7" E	Avicennia alba	1092
			Avicennia officinalis	796
			Excoecariaa agallocha	294
			Bruguiera gymnorrhiza	259
			Ceriops decandra	127
Sagar Island	Hooghly	21˚46'15.2" N 88˚10'09.3" E	Avicennia alba	722
			Avicennia officinalis	311
			Excoecariaa agallocha	244
			Bruguiera gymnorrhiza	355
			Sonneratia apetala	1044
Maipith	Matla	21˚51'58.3" N 88˚30'39.7" E	Avicennia alba	703
			Avicennia officinalis	444
			Bruguiera gymnorrhiza	333
			Avicennia marina	244
			Sonneratia apetala	277

4. Discussion

4.1. Soil Carbon Distribution across Depths

The observed depth-wise decline in total carbon (TC) and soil organic carbon (SOC) across all degraded mangrove sites reflects well-established patterns of organic matter dynamics in mangrove ecosystems. Surface soils (0 - 1 m), particularly at Maipith (Matla estuarine), exhibited the highest TC and SOC concentrations. This finding aligns with global studies (Ragavan et al., 2023; Wang et al., 2024b), which emphasize the critical role of mangrove vegetation in enriching surface soils with organic carbon. The higher carbon stocks at Maipith can be attributed to its dense mangrove vegetation, which promotes substantial organic matter inputs through litter deposition and root biomass accumulation (Nayak et

al., 2024). This enhances organic carbon preservation in surface soils, aligning with the observed elevated TC and SOC values in Maipith. The progressive decline in TC and SOC with depth reflects reduced organic matter inputs and enhanced mineralization and geochemical alteration in deeper layers. These trends are corroborated by earlier studies (Hicks Pries et al., 2023; Qin et al., 2024) who reported similar depth-wise carbon losses in tropical mangrove systems.

However, site-specific variations in carbon stocks likely stem from differences in vegetation density, sedimentation rates, and tidal inundation patterns, which govern organic matter deposition and preservation (Padhy et al., 2022). For example, higher SOC concentrations across depths at Maipith (Matla estuarine) may be attributed to better sediment trapping and prolonged tidal inundation, which enhance organic carbon burial and preservation. Anthropogenic activities, including industrial effluent discharge and land-use changes, further aggravate carbon losses in degraded mangroves (Bhattacharyya et al., 2023; Sharma et al., 2021).

4.2. Variation of Oxide Composition and Concentration

The predominance of silicon dioxide (SiO_2) across all depths at all three sites emphasizes the sedimentary nature of mangrove soils, with its increasing concentration at deeper layers indicating reduced organic inputs and greater mineral dominance. This trend aligns with earlier studies (Chen et al., 2025; Marchand, 2017), which highlight the role of silicate-rich sediment deposition in mangrove ecosystems. Higher SiO_2 concentrations in deeper soils at Maipith (Matla estuarine) and Sagar Island (Hooghly estuarine) reflect enhanced sedimentation processes and lower biological activity in these layers.

Ferric oxide (Fe_2O_3) concentration is highest in surface soils across all three sites, suggesting its pivotal role in stabilizing organic carbon through co-precipitation and adsorption mechanisms. This observation is consistent with findings (Ruiz et al., 2024), which emphasized the contribution of Fe_2O_3 to organic carbon preservation in mangrove soils. The depth-wise decline in Fe_2O_3 suggests redox-driven mobilization of iron under anoxic conditions, which is characteristic of water-logged mangrove environments (Cheng et al., 2021). This mobilization may lead to decreased iron availability for organic carbon stabilization in deeper layers.

The relatively stable concentrations of aluminium oxide (Al_2O_3) and potassium oxide (K_2O) across depths highlight their significance in forming clay-humus complexes, which contribute to long-term carbon stabilization. Similar patterns have been observed in mangrove systems globally (Wang et al., 2024b).

The minor fluctuations in magnesium oxide (MgO), sodium oxide (Na_2O), and calcium oxide (CaO) indicate relatively stable geochemical conditions in deeper layers, as suggested by (Das et al., 2023). The sharp decline in Na_2O with depth across all sites may result from reduced contributions from tidal inundation in subsurface soils. These findings highlight the influence of site-specific geochemical and hydrological factors in shaping the vertical distribution of major oxides (Chen et al., 2025; Qin et al., 2024).

The observed correlations between Soil Organic Carbon (SOC) and major oxides highlight the complex geochemical interactions governing carbon stabilization in Sundarbans mangrove soils. The strong positive correlation between SOC and Fe_2O_3 indicates the role of iron oxides in promoting long-term carbon sequestration. In mangrove ecosystems, the dynamic redox environment enhances the formation of Fe-organic matter complexes via mechanisms such as co-precipitation and ligand exchange, effectively protecting SOC from microbial decomposition.

The moderate positive correlation with SO_3 suggests a potential link between sulphur-bearing compounds and organic matter dynamics. In anaerobic environments like mangrove sediments, sulphur may contribute to SOC stabilization through the formation of organo-sulphur compounds or indirectly via iron-sulphide complexation. Additionally, the presence of sulphates can support microbial sulfate reduction, which may enhance the preservation of organic matter under reducing conditions.

The weak positive correlation between SOC and MnO supports the secondary role of manganese oxides in SOC stabilization. Like iron, manganese participates in redox reactions, albeit to a lesser extent, contributing to transient organic matter protection during redox cycling. Al_2O_3, showing a weak but positive trend, points to its role in stabilizing SOC through sorption processes and the formation of organo-metallic complexes, particularly in acidic, weathered tropical soils where aluminosilicate clays dominate. In contrast, the negative correlation between SOC and SiO_2 suggests that sandy, quartz-rich sediments—typical of deltaic environments—have a diminished capacity to retain organic carbon due to low surface reactivity and limited formation of stable mineral-organic associations.

Overall, these relationships suggest that iron, sulphur, and to a lesser extent, aluminium and manganese oxides, contribute to the geochemical stabilization of SOC in mangrove soils.

4.3. Trace Elements Composition and Concentrations

The depth-wise distribution of trace elements across the three studied sites, namely Maipith (Matla estuarine), Sagar Island (Hooghly estuarine), and Dayapur (Bidyadhari estuarine), revealed significant spatial and geochemical variations shaped predominantly by anthropogenic activities, with tidal and geological influences playing secondary roles (Ghosh et al., 2024).

At Maipith (Matla estuarine), surface soils (0 - 1 m) showed moderate Cr and Mn concentrations, which declined sharply with depth. The relatively low Mn levels suggest limited tidal inundation and reduced sediment trapping compared to the other sites (Madi et al., 2015; Mapanao-Villar et al., 2024). Ni and Cu concentrations followed a similar trend, with Cu stabilizing at mid-depths, likely due to clay-organic complexation (Rahman et al., 2024). Elevated Cd levels at intermediate depths indicate sulphide phase formation under reducing conditions, consistent with localized geochemical stability (Robin et al., 2024).

Sagar Island (Hooghly estuarine) exhibited the highest trace element concentrations across all depths, suggesting significant anthropogenic inputs combined with efficient sediment trapping under prolonged tidal inundation (Fu et al., 2023; Ghosh et al., 2024). Surface Mn (696.10 ppm) and Cr (89.13 ppm) levels were among the highest, with Mn peaking at 1 - 2 m (787.76 ppm). The higher concentrations of Mn and Cr at mid-depths suggests active redox cycling facilitated by anthropogenic sediment contributions (Akhand et al., 2024; Mapanao-Villar et al., 2024). Ni and Cu levels peaked at 2 - 3 m, likely due to stabilization by clay minerals and organic matter, while Cd concentrations peaked at mid-depths (16.83 ppm), consistent with redox-driven sulphide formation (Guo et al., 2023; Islam et al., 2023).

Dayapur (Bidyadhari estuarine) exhibited significant surface-level enrichment of Zn and Pb, indicative of substantial anthropogenic inputs, such as agricultural runoff and industrial effluents (Badawy et al., 2024; Tang et al., 2022). With depth, Zn and Pb concentrations declined sharply, while the lowest Mn concentrations (241.65 ppm at 4 - 5 m) indicates reduced sedimentation rates and limited tidal influence (Chakraborty, 2024).

Overall, the site-specific variations highlight the dynamic relationship between redox conditions, tidal regimes, and anthropogenic inputs, with anthropogenic influences emerging as the dominant factor shaping trace element distributions across all sites (Pavoni et al., 2021). The anthropogenic impact at Dayapur (Bidyadhari estuarine), although lower than at Sagar Island, is more pronounced than at Maipith (Matla estuarine), further emphasizing the dominance of human activities over natural tidal processes in influencing trace element distributions (Selvaraj et al., 2024). Elevated surface levels of Zn and Pb highlight the urgent need for regulating human activities, particularly at Sagar Island (Hooghly estuarine) and Dayapur (Bidyadhari estuarine).

The correlation analysis between Soil Organic Carbon (SOC) and trace elements in Sundarban mangrove soils reveals specific patterns that offer insights into biogeochemical interactions influencing carbon dynamics. The moderate positive correlation between SOC and Copper (Cu) ($r \approx 0.43$) suggests that Cu may play a contributory role in SOC stabilization. Copper is known to participate in microbial enzymatic processes and has a strong affinity for humic substances, often forming stable organo-metallic complexes (Fu et al., 2023). Nickel (Ni), exhibiting a positive correlation with SOC ($r \approx 0.26$), may indicate partial association with organic matter. Though typically considered a lithogenic or mineral-associated element, Ni can interact with organic ligands under certain pH and redox conditions.

On the other hand, the weak or negligible correlations observed between SOC and Manganese (Mn), Zinc (Zn), and Lead (Pb) suggest limited geochemical or biological coupling in this context. These elements may be present in forms not readily complexed with organic matter or may be governed by separate geochemical pathways. For instance, Mn is redox-sensitive and may be more influenced by

oxidation-reduction dynamics than organic matter content (Badawy et al., 2024; Islam et al., 2023). Similarly, Zn and Pb, despite known complexation potentials, may preferentially associate with inorganic mineral phases or precipitate under prevailing soil conditions, thereby weakening their correlation with SOC (Chakraborty, 2024).

Overall, the modest positive correlations with Cu and Ni imply selective trace element roles in SOC dynamics, while the lack of correlation with Mn, Zn, and Pb highlights the complexity of trace metal behaviour in estuarine mangrove systems.

4.4. Variation of Clay Mineral Composition

The presence of glauconite in shallow soils (1 m depth) across all three estuarine systems explains the influence of saline water intrusion and tidal dynamics. Glauconite formation in such environments is facilitated by sodium ion exchange, as previously reported in saline coastal soils (Choudhury et al., 2022). This uniformity across sites indicates a common geochemical process. At greater depths (5 m), the detection of argentopyrite and pyrite indicates the possibility of sulphate reduction under anoxic conditions. These minerals are indicative of active sulphur cycling and organic matter decomposition, consistent with reducing environments found in water-logged soils.

In Dayapur (Bidyadhari estuarine), the detection of zinnwaldite at 2.5 m depth suggests lithogenic contributions or weathering of mica-rich parent materials, emphasizing the influence of local geology. The presence of sepiolite at 5 m depth further reflects prolonged water stagnation and alkaline soil conditions, likely driven by magnesium leaching under constrained hydrology (El Rasafi et al., 2024; Hamid et al., 2021). In Sagar Island (Hooghly estuarine), tamarugite (sodium and aluminium-rich sulphate hydrate) at 5 m signifies extreme salinity and acidic conditions driven by seawater and brine deposits. In Maipith (Matla estuarine), the detection of chlorite-vermicullite at 1m depth indicates partial weathering of chlorite under alternating wet and dry conditions (Wang et al., 2021), while the presence of argentopyrite and montmorillonite at 5m depth highlights reducing conditions and sedimentation processes that favour fine-grained clay accumulation (Ferreira et al., 2022). These mineral transformations are indicative of dynamic redox conditions and sediment deposition patterns in mangrove ecosystems.

4.5. Mangrove Species Distribution and Density Patterns across Estuarine Systems

The observed variation in mangrove species composition and density across the three estuarine sites highlights the ecological heterogeneity of the Indian Sundarbans. The dominance of *Avicennia alba* across all sites, particularly at Dayapur, suggests its broad ecological tolerance and adaptive capacity to varying salinity and tidal regimes. The exclusive presence of *Ceriops decandra* at Dayapur and *Avicennia marina* at Maipith further indicates the influence of site-specific microenvironmental conditions such as soil salinity, hydrology, and sediment

characteristics on species distribution.

Sagar Island, with the highest total vegetation density, is dominated by *Sonneratia apetala*, a fast-growing species known for its tolerance to dynamic estuarine environments and potential contribution to biomass accumulation. This dense vegetation cover may enhance organic matter input to the soil, indirectly influencing soil organic carbon (SOC) accumulation and stabilization through increased litter deposition and root biomass (Nayak et al., 2024).

While this study primarily focuses on geochemical controls of carbon sequestration, incorporating biotic data provides a more integrated understanding of SOC dynamics. Variations in species-specific traits—such as litter quality and biomass productivity—can significantly modulate the input, composition, and turnover of organic matter in mangrove soils. These insights highlight the importance of considering vegetation structure alongside geochemical parameters to better evaluate carbon sequestration potential in mangrove ecosystems.

5. Conclusion

Our study showed that there was not much geological influence on the soil organic carbon storage and stability of SOC. Surface soils serve as active carbon accumulation zones due to mangrove litter and root biomass, while deeper layers act as long-term carbon reservoirs, safeguarded by anoxic conditions that inhibit decomposition. This signifies the importance of both surface and subsurface soils in mangrove carbon dynamics. SiO_2 concentrations was higher at greater depths across all three estuarine systems. Hooghly estuary showed higher surface Fe_2O_3 concentration and moderate SiO_2 concentration. Bidyadhari estuary had the lowest SiO_2 and Fe_2O_3 concentrations but the highest surface Al_2O_3, which increased with depth. Sedimentation effects were found to be negligible except in the case of copper (Cu) concentration, where localized sedimentary processes may have influenced trace element deposition. The concentration of chromium (Cr) and lead (Pb) was clearly influenced by anthropogenic activities in the study area, indicating the trends observed in these two trace elements. Despite these influences, all toxic trace elements, including cadmium (Cd) and lead (Pb), were found to be within permissible limits as per environmental safety standards, suggesting minimal immediate ecological risks while highlighting the resilience of the Sundarban mangrove soils to contamination. Overall, this study emphasizes the important role of Sundarban degraded mangrove ecosystem in global carbon sequestration and the need for site-specific conservation and management strategies. Future research should integrate geochemical modelling and long-term monitoring to fully leverage the carbon sequestration potential of these unique degraded mangrove systems, which have become an integral part of the wetland ecosystem, contributing to climate change mitigation and sustainable ecosystem management.

Conflicts of Interest

The authors declare no conflicts of interest regarding the publication of this paper.

References

Akhand, A., Liu, H., Ghosh, A., Chanda, A., Dasgupta, R., Mishrra, S. et al. (2024). Application of Structural Equation Modelling to Study Complex "Blue Carbon" Cycling in Mangrove Ecosystems. *Marine Pollution Bulletin, 209,* Article 117290. https://doi.org/10.1016/j.marpolbul.2024.117290

Al Mahmud, J., Siraz, M. M. M., Alam, M. S., Dewan, M. J., Rashid, M. B., Khandaker, M. U. et al. (2024). A Pioneering Study of the Radiological Mapping in the World's Largest Mangrove Forest (The Sundarbans) and Implications for the Public and Environment. *Marine Pollution Bulletin, 202,* Article 116349. https://doi.org/10.1016/j.marpolbul.2024.116349

Alongi, D. M. (2012). Carbon Sequestration in Mangrove Forests. *Carbon Management, 3,* 313-322. https://doi.org/10.4155/cmt.12.20

Badawy, W. M., Dmitriev, A. Y., El Samman, H., El-Taher, A., Blokhin, M. G., Rammah, Y. S. et al. (2024). Elemental Composition and Metal Pollution in Egyptian Red Sea Mangrove Sediments: Characterization and Origin. *Marine Pollution Bulletin, 198,* Article 115830. https://doi.org/10.1016/j.marpolbul.2023.115830

Bhattacharyya, P., Padhy, S. R., Khanam, R., Nayak, A. K., Dash, P. K., Reddy, C. S. et al. (2023). Marine Estuaries Act as Better Sink for Greenhouse Gases during Winter in Undisturbed Mangrove than Degraded Ones in Sundarban, India. *Marine Environmental Research, 191,* Article 106147. https://doi.org/10.1016/j.marenvres.2023.106147

Cai, C., Anton, A., Duarte, C. M., & Agusti, S. (2024). Spatial Variations of Nutrient and Trace Metal Concentrations in Macroalgae across Blue Carbon Habitats of the Saudi Arabian Red Sea. *Science of The Total Environment, 956,* Article 177197. https://doi.org/10.1016/j.scitotenv.2024.177197

Chakraborty, D. (2024). Mangroves as an Effective Tool of Phytoremediation and Its Implications on Agricultural Land in Estuarine Zones. In N. K. Singh, S. Afzal, & T. Aftab (Eds.), *Phytoremediation and Biofortification* (pp. 131-146). Apple Academic Press. https://doi.org/10.1201/9781003402084-6

Chen, Z. L., Zhang, Z., Cai, R., Yi, Y., Liang, W., Macreadie, P. I. et al. (2025). Molecular Fingerprints of Sedimentary Dissolved Organic Matter in Mangroves: Importance to Blue Carbon Sequestration. *Chemical Geology, 671,* Article 122495. https://doi.org/10.1016/j.chemgeo.2024.122495

Cheng, Q., Jiang, H., Jin, Z., Jiang, Y., Hui, C., Xu, L. et al. (2021). Effects of Fe_2O_3 Nanoparticles on Extracellular Polymeric Substances and Nonylphenol Degradation in River Sediment. *Science of The Total Environment, 770,* Article 145210. https://doi.org/10.1016/j.scitotenv.2021.145210

Choudhary, B., Dhar, V., & Pawase, A. S. (2024). Blue Carbon and the Role of Mangroves in Carbon Sequestration: Its Mechanisms, Estimation, Human Impacts and Conservation Strategies for Economic Incentives. *Journal of Sea Research, 199,* Article 102504. https://doi.org/10.1016/j.seares.2024.102504

Choudhury, T. R., Khanolkar, S., & Banerjee, S. (2022). Glauconite Authigenesis during the Warm Climatic Events of Paleogene: Case Studies from Shallow Marine Sections of Western India. *Global and Planetary Change, 214,* Article 103857. https://doi.org/10.1016/j.gloplacha.2022.103857

Cooray, I. G., Chalmers, G., & Chittleborough, D. (2024). The Impact of Sampling Depths on Quantification of Soil Organic Carbon Stock in Mangrove Environments. *CATENA, 246,* Article 108398. https://doi.org/10.1016/j.catena.2024.108398

Das, A., Purakayastha, T. J., Ahmed, N., Das, R., Biswas, S., Shivay, Y. S. et al. (2023). Influence of Clay Mineralogy on Soil Organic Carbon Stabilization under Tropical Cli-

mate, India. *Journal of Soil Science and Plant Nutrition, 23,* 1003-1018. https://doi.org/10.1007/s42729-022-01099-x

Donato, D. C., Kauffman, J. B., Murdiyarso, D., Kurnianto, S., Stidham, M., & Kanninen, M. (2011). Mangroves among the Most Carbon-Rich Forests in the Tropics. *Nature Geoscience, 4,* 293-297. https://doi.org/10.1038/ngeo1123

El Rasafi, T., El Moukhtari, A., Farissi, M., Ziouti, A., Prasad, M. N. V., Oukarroum, A. et al. (2024). Soil Amendments as Promising Strategies for Phytomanagement of Cd Contaminated Soils. In A. Husen, M. Iqbal, A. Ditta, S. Mehmood, M. Imtiaz, & M. S. Tu (Eds.), *Bio-Organic Amendments for Heavy Metal Remediation* (pp. 499-513). Elsevier. https://doi.org/10.1016/b978-0-443-21610-7.00041-0

Ferreira, T. O., Queiroz, H. M., Nóbrega, G. N., de Souza Júnior, V. S., Barcellos, D., Ferreira, A. D. et al. (2022). Litho-Climatic Characteristics and Its Control over Mangrove Soil Geochemistry: A Macro-Scale Approach. *Science of The Total Environment, 811,* Article 152152. https://doi.org/10.1016/j.scitotenv.2021.152152

Frates, E. S., Spietz, R. L., Silverstein, M. R., Girguis, P., Hatzenpichler, R., & Marlow, J. J. (2023). Natural and Anthropogenic Carbon Input Affect Microbial Activity in Salt Marsh Sediment. *Frontiers in Microbiology, 14,* Article 1235906. https://doi.org/10.3389/fmicb.2023.1235906

Fu, C., Li, Y., Tu, C., Hu, J., Zeng, L., Qian, L. et al. (2023). Dynamics of Trace Element Enrichment in Blue Carbon Ecosystems in Relation to Anthropogenic Activities. *Environment International, 180,* Article 108232. https://doi.org/10.1016/j.envint.2023.108232

Ghosh, A., Baidya, S., & Gupta, A. K. (2024). Climate Change Impact on Landuse and Livelihood in Sundarbans: A Case Study of Sagar Island. In A. K. Gupta, A. Gupta, & P. Acharya (Eds.), *Disaster Resilience and Green Growth* (pp. 403-434). Springer Nature. https://doi.org/10.1007/978-981-99-4105-6_20

Grey, A., Costeira, R., Lorenzo, E., O'Kane, S., McCaul, M. V., McCarthy, T. et al. (2023). Geochemical Properties of Blue Carbon Sediments through an Elevation Gradient: Study of an Anthropogenically Impacted Coastal Lagoon. *Biogeochemistry, 162,* 381-408. https://doi.org/10.1007/s10533-022-00974-0

Guo, Z., Liu, J., Zeng, H., Xiao, X., Liu, M., Hong, H. et al. (2023). Variation of Glomalin-Metal Binding Capacity in 1 M Soil Profiles from Mangrove Forests to Mudflat and Affected Factor Analysis. *Science of The Total Environment, 863,* Article 160890. https://doi.org/10.1016/j.scitotenv.2022.160890

Hamid, Y., Tang, L., Hussain, B., Usman, M., Liu, L., Ulhassan, Z. et al. (2021). Sepiolite Clay: A Review of Its Applications to Immobilize Toxic Metals in Contaminated Soils and Its Implications in Soil-Plant System. *Environmental Technology & Innovation, 23,* Article 101598. https://doi.org/10.1016/j.eti.2021.101598

Hicks Pries, C. E., Ryals, R., Zhu, B., Min, K., Cooper, A., Goldsmith, S. et al. (2023). The Deep Soil Organic Carbon Response to Global Change. *Annual Review of Ecology, Evolution, and Systematics, 54,* 375-401. https://doi.org/10.1146/annurev-ecolsys-102320-085332

Islam, M. M., Akther, S. M., Hossain, M. F., & Parveen, Z. (2022). Spatial Distribution and Ecological Risk Assessment of Potentially Toxic Metals in the Sundarbans Mangrove Soils of Bangladesh. *Scientific Reports, 12,* Article No. 10422. https://doi.org/10.1038/s41598-022-13609-z

Islam, M. M., Akther, S. M., Wahiduzzaman, M., Hossain, M. F., & Parveen, Z. (2023). Fractionation and Contamination Assessment of Zn, Cu, Fe, and Mn in the Sundarbans Mangrove Soils of Bangladesh. *Soil and Sediment Contamination: An International*

Journal, 32, 789-811. https://doi.org/10.1080/15320383.2022.2142513

Kauffman, J. B., Adame, M. F., Arifanti, V. B., Schile-Beers, L. M., Bernardino, A. F., Bhomia, R. K. et al. (2020). Total Ecosystem Carbon Stocks of Mangroves across Broad Global Environmental and Physical Gradients. *Ecological Monographs, 90,* e01405. https://doi.org/10.1002/ecm.1405

Li, Q., Hu, W., Li, L., & Li, Y. (2023). Interactions between Organic Matter and Fe Oxides at Soil Micro-Interfaces: Quantification, Associations, and Influencing Factors. *Science of The Total Environment, 855,* Article 158710. https://doi.org/10.1016/j.scitotenv.2022.158710

Madi, A. P. L. M., Boeger, M. R. T., & Reissmann, C. B. (2015). Distribution of Cu, Fe, Mn, and Zn in Two Mangroves of Southern Brazil. *Brazilian Archives of Biology and Technology, 58,* 970-976. https://doi.org/10.1590/s1516-89132015060255

Mapanao-Villar, K., Abella, G. P., Pakaigue-Valera, M., Villen, J. W., & Ponce, C. D. (2024). Mangroves and Their Associates in Metal-Rich Soils in Candelaria, Zambales Province, Philippines. *Journal of Environmental Science and Management, 27,* 80-89. https://doi.org/10.47125/jesam/2024_1/07

Marchand, C. (2017). Soil Carbon Stocks and Burial Rates along a Mangrove Forest Chronosequence (French Guiana). *Forest Ecology and Management, 384,* 92-99. https://doi.org/10.1016/j.foreco.2016.10.030

Murugesan, A., Loganathan, M., Senthil Kumar, P., & Vo, D. N. (2021). Cobalt and Nickel Oxides Supported Activated Carbon as an Effective Photocatalysts for the Degradation Methylene Blue Dye from Aquatic Environment. *Sustainable Chemistry and Pharmacy, 21,* Article 100406. https://doi.org/10.1016/j.scp.2021.100406

Nayak, S. K., Bhattacharyya, P., Padhy, S. R., Das, A., & Parida, S. P. (2024). Spatial Variation of Algal Diversity Due to Conversion of Mangrove to Rice Ecology in Sundarban, India. *Biodiversity and Conservation, 34,* 191-206. https://doi.org/10.1007/s10531-024-02965-z

Padhy, S. R., Bhattacharyya, P., Dash, P. K., Nayak, S. K., Das, A., Parida, S. P. et al. (2023). Comparative Accounting of Methane and Nitrous Oxide Fluxes with Related Soil Parameters of Degraded Mangrove Wetlands and Adjacent Rice Fields in Sundarban, India. *Atmospheric Pollution Research, 14,* Article 101749. https://doi.org/10.1016/j.apr.2023.101749

Padhy, S. R., Bhattacharyya, P., Dash, P. K., Nayak, S. K., Parida, S. P., Baig, M. J. et al. (2022). Elucidation of Dominant Energy Metabolic Pathways of Methane, Sulphur and Nitrogen in Respect to Mangrove-Degradation for Climate Change Mitigation. *Journal of Environmental Management, 303,* Article 114151. https://doi.org/10.1016/j.jenvman.2021.114151

Padhy, S. R., Bhattacharyya, P., Dash, P. K., Reddy, C. S., Chakraborty, A., & Pathak, H. (2020). Seasonal Fluctuation in Three Mode of Greenhouse Gases Emission in Relation to Soil Labile Carbon Pools in Degraded Mangrove, Sundarban, India. *Science of The Total Environment, 705,* Article 135909. https://doi.org/10.1016/j.scitotenv.2019.135909

Padhy, S. R., Bhattacharyya, P., Nayak, S. K., Dash, P. K., & Mohapatra, T. (2021). A Unique Bacterial and Archaeal Diversity Make Mangrove a Green Production System Compared to Rice in Wetland Ecology: A Metagenomic Approach. *Science of The Total Environment, 781,* Article 146713. https://doi.org/10.1016/j.scitotenv.2021.146713

Pavoni, E., Crosera, M., Petranich, E., Faganeli, J., Klun, K., Oliveri, P. et al. (2021). Distribution, Mobility and Fate of Trace Elements in an Estuarine System under Anthropogenic Pressure: The Case of the Karstic Timavo River (Northern Adriatic Sea, Italy). *Estuaries and Coasts, 44,* 1831-1847. https://doi.org/10.1007/s12237-021-00910-9

Qin, G., Lu, Z., Gan, S., Zhang, L., Zhang, J., Zhou, J. et al. (2024). Fate of Soil Organic Carbon in Estuarine Mangroves: Evidences from Stable Isotopes and Lignin Biomarkers. *CATENA, 246,* Article 108401. https://doi.org/10.1016/j.catena.2024.108401

Queiroz, H. M., Ferreira, T. O., Fandiño, V. A., Bragantini, I. O. B. F., Barcellos, D., Nóbrega, G. N. et al. (2022). Changes in Soil Iron Biogeochemistry in Response to Mangrove Dieback. *Biogeochemistry, 158,* 357-372. https://doi.org/10.1007/s10533-022-00903-1

Ragavan, P., Rahman, A., Sarkar, S., Verma, S., Jeeva, C., Mohan, P. M. et al. (2023). Variability in Soil Organic Carbon Stock and Isotopic Signature in Tropical Island Mangrove Forests of India. *Regional Environmental Change, 23,* Article No. 135. https://doi.org/10.1007/s10113-023-02130-2

Rahman, S. U., Han, J., Zhou, Y., Ahmad, M., Li, B., Wang, Y. et al. (2024). Adaptation and Remediation Strategies of Mangroves against Heavy Metal Contamination in Global Coastal Ecosystems: A Review. *Journal of Cleaner Production, 441,* Article 140868. https://doi.org/10.1016/j.jclepro.2024.140868

Ray, A., Kumar, M., Karim, A. A., Biswas, K., & Sarkar, B. (2023). Chromium Contamination in Soil from Mining Activities: A Constraint for Crop Production and Potential Mitigation Strategies. In N. Bolan, & M. B. Kirkham (Eds.), *Soil Constraints and Productivity* (pp. 83-99). CRC Press. https://doi.org/10.1201/9781003093565-5

Ray, R., Chowdhury, C., Majumder, N., Dutta, M. K., Mukhopadhyay, S. K., & Jana, T. K. (2013). Improved Model Calculation of Atmospheric CO_2 Increment in Affecting Carbon Stock of Tropical Mangrove Forest. *Tellus B: Chemical and Physical Meteorology, 65,* Article 18981. https://doi.org/10.3402/tellusb.v65i0.18981

Ray, R., Mandal, S. K., González, A. G., Pokrovsky, O. S., & Jana, T. K. (2021). Storage and Recycling of Major and Trace Element in Mangroves. *Science of The Total Environment, 780,* Article 146379. https://doi.org/10.1016/j.scitotenv.2021.146379

Robin, S. L., Baudin, F., Le Milbeau, C., & Marchand, C. (2024). Millennial-Aged Organic Matter Preservation in Anoxic and Sulfidic Mangrove Soils: Insights from Isotopic and Molecular Analyses. *Estuarine, Coastal and Shelf Science, 308,* Article 108936. https://doi.org/10.1016/j.ecss.2024.108936

Romero-Mujalli, G., & Melendez, W. (2023). Nutrients and Trace Elements of Semi-Arid Dwarf and Fully Developed Mangrove Soils, Northwestern Venezuela. *Environmental Earth Sciences, 82,* Article No. 51. https://doi.org/10.1007/s12665-022-10701-5

Rovai, A. S., Twilley, R. R., Castañeda-Moya, E., Riul, P., Cifuentes-Jara, M., Manrow-Villalobos, M. et al. (2018). Global Controls on Carbon Storage in Mangrove Soils. *Nature Climate Change, 8,* 534-538. https://doi.org/10.1038/s41558-018-0162-5

Royna, M., Murdiyarso, D., Sasmito, S. D., Arriyadi, D., Rahajoe, J. S., Zahro, M. G. et al. (2024). Carbon Stocks and Effluxes in Mangroves Converted into Aquaculture: A Case Study from Banten Province, Indonesia. *Frontiers in Ecology and Evolution, 12,* Article 1340531. https://doi.org/10.3389/fevo.2024.1340531

Ruiz, F., Bernardino, A. F., Queiroz, H. M., Otero, X. L., Rumpel, C., & Ferreira, T. O. (2024). Iron's Role in Soil Organic Carbon (de)Stabilization in Mangroves under Land Use Change. *Nature Communications, 15,* Article No. 10433. https://doi.org/10.1038/s41467-024-54447-z

Selvaraj, V., Pandu, P., Saradhambal, S. R., Sankarappan, R., & Anandarao, R. (2024). An Appraisal of Trace Element Concentration and Environmental Risk of Sediments: A Baseline Study of Sediments from Arasalar River Estuary, Tamil Nadu, India. *Environmental Science and Pollution Research, 31,* 41446-41461. https://doi.org/10.1007/s11356-023-28552-3

Sharma, D., Rao, K., & Ramanathan, A. (2021). A Systematic Review on the Impact of Urbanization and Industrialization on Indian Coastal Mangrove Ecosystem. In S. Madhav, S. Nazneen, & P. Singh (Eds.), *Coastal Research Library* (pp. 175-199). Springer International Publishing. https://doi.org/10.1007/978-3-030-84255-0_8

Sierra, C. A., Ahrens, B., Bolinder, M. A., Braakhekke, M. C., von Fromm, S., Kätterer, T. et al. (2024). Carbon Sequestration in the Subsoil and the Time Required to Stabilize Carbon for Climate Change Mitigation. *Global Change Biology, 30,* e17153. https://doi.org/10.1111/gcb.17153

Spalding, M. (2010). *World Atlas of Mangroves*. Routledge.

Tang, D., Luo, S., Deng, S., Huang, R., Chen, B., & Deng, Z. (2022). Heavy Metal Pollution Status and Deposition History of Mangrove Sediments in Zhanjiang Bay, China. *Frontiers in Marine Science, 9,* Article 989584. https://doi.org/10.3389/fmars.2022.989584

Tognella, M. M. P., Soares, M. L. G., Cuevas, E., & Medina, E. (2016). Heterogeneity of Elemental Composition and Natural Abundance of Stables Isotopes of C and N in Soils and Leaves of Mangroves at Their Southernmost West Atlantic Range. *Brazilian Journal of Biology, 76,* 994-1003. https://doi.org/10.1590/1519-6984.05915

Wang, Q., Wen, Y., Zhao, B., Hong, H., Liao, R., Li, J. et al. (2021). Coastal Soil Texture Controls Soil Organic Carbon Distribution and Storage of Mangroves in China. *CATENA, 207,* Article 105709. https://doi.org/10.1016/j.catena.2021.105709

Wang, W., Chen, C., Huang, X., Jiang, S., Xiong, J., Li, J. et al. (2024a). Chromium(VI) Adsorption and Reduction in Soils under Anoxic Conditions: The Relative Roles of Iron (Oxyhr)Oxides, Iron(II), Organic Matters, and Microbes. *Environmental Science & Technology, 58,* 18391-18403. https://doi.org/10.1021/acs.est.4c08677

Wang, X., Wang, C., Fan, X., Sun, L., Sang, C., Wang, X. et al. (2024b). Mineral Composition Controls the Stabilization of Microbially Derived Carbon and Nitrogen in Soils: Insights from an Isotope Tracing Model. *Global Change Biology, 30,* e17156. https://doi.org/10.1111/gcb.17156

Wu, S., Li, H., Yuan, B., Chen, X., He, L., Li, Q. et al. (2024). Regulation of Precipitation on Soil Dissolved Organic Matter in Perturbed Mangrove Ecosystems. *Ecosystem Health and Sustainability, 10,* Article ID: 0156. https://doi.org/10.34133/ehs.0156